

# The selective effect of environment on the atomic and molecular gas-to-dust ratio of nearby galaxies in the *Herschel* Reference Survey

L. Cortese,<sup>1\*</sup> K. Bekki,<sup>1</sup> A. Boselli,<sup>2</sup> B. Catinella,<sup>1</sup> L. Ciesla,<sup>3</sup> T. M. Hughes,<sup>4</sup>  
M. Baes,<sup>5</sup> G. J. Bendo,<sup>6</sup> M. Boquien,<sup>7</sup> I. de Looze,<sup>8</sup> M. W. L. Smith,<sup>9</sup>  
L. Spinoglio<sup>10</sup> and S. Viaene<sup>5</sup>

<sup>1</sup>International Centre for Radio Astronomy Research, The University of Western Australia, 35 Stirling Hwy, Crawley, WA 6009, Australia

<sup>2</sup>Aix Marseille Université, CNRS, LAM (Laboratoire d'Astrophysique de Marseille) UMR 7326, F-13388, Marseille, France

<sup>3</sup>Laboratoire AIM, CEA/DSM/IRFU, CNRS, Université Paris-Diderot, F-91190 Gif, France

<sup>4</sup>Instituto de Física y Astronomía, Universidad de Valparaíso, Avda. Gran Bretaña 1111, Valparaíso, Chile

<sup>5</sup>Sterrenkundig Observatorium, Universiteit Gent, Krijgslaan 281, B-9000 Gent, Belgium

<sup>6</sup>UK ALMA Regional Centre Node, Jodrell Bank Centre for Astrophysics, School of Physics and Astronomy, The University of Manchester, Oxford Road, Manchester M13 9PL, UK

<sup>7</sup>Unidad de Astronomía, Fac. Cs Básicas, Universidad de Antofagasta, Avda. U. de Antofagasta 02800, Antofagasta, Chile

<sup>8</sup>Department of Physics and Astronomy, University College London, Gower Street, London WC1E 6BT, UK

<sup>9</sup>School of Physics and Astronomy, Cardiff University, The Parade, Cardiff CF24 3AA, UK

<sup>10</sup>Istituto di Astrofisica e Planetologia Spaziali, INAF, Via del Fosso del Cavaliere 100, I-00133 Roma, Italy

Accepted 2016 April 5. Received 2016 March 30; in original form 2015 December 2

## ABSTRACT

We combine dust, atomic (H I) and molecular (H<sub>2</sub>) hydrogen mass measurements for 176 galaxies in the *Herschel* Reference Survey to investigate the effect of environment on the gas-to-dust mass ( $M_{\text{gas}}/M_{\text{dust}}$ ) ratio of nearby galaxies. We find that, at fixed stellar mass, the average  $M_{\text{gas}}/M_{\text{dust}}$  ratio varies by no more than a factor of  $\sim 2$  when moving from field to cluster galaxies, with Virgo galaxies being slightly more dust rich (per unit of gas) than isolated systems. Remarkably, once the molecular and atomic hydrogen phases are investigated separately, we find that H I-deficient galaxies have at the same time lower  $M_{\text{H I}}/M_{\text{dust}}$  ratio but higher  $M_{\text{H}_2}/M_{\text{dust}}$  ratio than H I-normal systems. In other words, they are poorer in atomic but richer in molecular hydrogen if normalized to their dust content. By comparing our findings with the predictions of theoretical models, we show that the opposite behaviour observed in the  $M_{\text{H I}}/M_{\text{dust}}$  and  $M_{\text{H}_2}/M_{\text{dust}}$  ratios is fully consistent with outside-in stripping of the interstellar medium (ISM), and is simply a consequence of the different distribution of dust, H I and H<sub>2</sub> across the disc. Our results demonstrate that the small environmental variations in the total  $M_{\text{gas}}/M_{\text{dust}}$  ratio, as well as in the gas-phase metallicity, do not automatically imply that environmental mechanisms are not able to affect the dust and metal content of the ISM in galaxies.

**Key words:** galaxies: clusters: general – galaxies: evolution – galaxies: fundamental parameters – intergalactic medium.

## 1 INTRODUCTION

The discovery, three decades ago, of a significant population of atomic hydrogen (H I) deficient galaxies in nearby clusters (i.e. systems with lower H I content than isolated galaxies of similar optical diameter and morphological type; Haynes & Giovanelli 1984; Giovanelli & Haynes 1985) provided the first clear observational

evidence for removal of the interstellar medium (ISM) in high-density environments.

Since then, thanks to the improvement of ground- and space-based facilities across the infrared to radio wavelength range, not only it has been possible to quantify more accurately the effect of the cluster environment on the H I content of galaxies (Solanes et al. 2001; Boselli & Gavazzi 2006; Cortese et al. 2011), but also we have started to show that environmental mechanisms can affect the other components of the ISM, such as molecular hydrogen (H<sub>2</sub>), dust, and metals (Cortese et al. 2012a; Hughes et al. 2013; Boselli

\* E-mail: [luca.cortese@uwa.edu.au](mailto:luca.cortese@uwa.edu.au)

et al. 2014b). Indeed, both large statistical studies and detailed investigations of peculiar galaxies (e.g. Vollmer et al. 2005, 2008; Fumagalli et al. 2009; Cortese et al. 2010a,b; Sivanandam, Rieke & Rieke 2010; Pappalardo et al. 2012; Jáchym et al. 2014; Kenney, Abramson & Bravo-Alfaro 2015; Scott et al. 2015) have shown that H I-deficient systems are also, at fixed stellar mass, H<sub>2</sub> and dust deficient when compared to isolated galaxies. However, the effect on dust grains and molecules appears to be less dramatic than in the case of H I supporting a scenario in which the ISM removal is more efficient in the outer, H I-dominated, star-forming disc (Cortese et al. 2010a, 2012a; Pappalardo et al. 2012; Boselli et al. 2014b), as expected in the case of hydrodynamical mechanisms, such as ram pressure (Gunn & Gott 1972).

Perhaps surprisingly, no or very little variation with environment is observed in the metal content of galaxies when this is quantified by means of the oxygen abundance (or gas-phase metallicity), which provides the amount of oxygen per unit of hydrogen in galaxies. Several works have now consistently shown that the variation in gas-phase metallicity (at fixed stellar mass) across environments is  $\sim 0.1$  dex at most (Mouhcine, Baldry & Bamford 2007; Ellison et al. 2009; Petropoulou, Vílchez & Iglesias-Páramo 2012; Hughes et al. 2013). This observational result may suggest that the cluster environment is not able to affect the metal content of galaxies, in contradiction with the evidence supporting ram-pressure stripping.

However, this could simply come down to the fact that gas, dust, and metal depletion by environment are usually quantified in different ways. While for gas and dust the amount of stripping is estimated by normalizing the mass of ISM to the stellar mass, the gas-phase metallicity gives us, by construction, the amount of metals per unit of hydrogen mass. Thus, it is easy to see how the gas-phase metallicity of galaxies may not change with environment even if both metals and gas are removed from disc. Unfortunately, as oxygen abundance estimates do not provide an absolute quantification of the total amount of metals in the ISM, they cannot be easily used to test this scenario.

The most promising way to make progress in this field is thus to investigate the effect of environment on the chemical enrichment of galaxies by using the gas-to-dust ratio, instead of oxygen abundance, as a proxy for the amount of metals per unit of hydrogen. Indeed, assuming that the dust formation and destruction time-scales are similar, it has been shown that the gas-to-dust ratio should scale with metallicity (Dwek 1998), as observed in nearby galaxies, although with significant scatter (Issa, MacLaren & Wolfendale 1990; Muñoz-Mateos et al. 2009; Magrini et al. 2011; Rémy-Ruyer et al. 2014).

This technique has several advantages when compared to the oxygen abundances derived from optical emission lines. First, by measuring independently the total amount of gas and dust in galaxies, and not just their ratios as in the case of oxygen abundance, it is easier to follow the effect of environment on each ISM component separately. Secondly, while active star formation is needed to estimate gas-phase metallicities, far-infrared dust continuum emission relies less on the presence of star-forming regions as a significant fraction of dust heating comes from evolved stellar populations (e.g. Boquien et al. 2011; Bendo et al. 2012, 2015). Thus, we can investigate the properties of the most environmentally perturbed galaxies, which are generally excluded from studies of the stellar mass versus metallicity relations simply because quiescent. Thirdly, thanks to the *Herschel Space Observatory* we are able to trace the dust distribution across the entire disc, whereas gas-phase metallicity estimates have so far been generally biased towards the central regions of galaxies (Hughes et al. 2013).

Until very recently, this kind of analysis was limited by the lack of dust and molecular hydrogen estimates for representative samples spanning galaxies in different environments. In the last few years, we have been able to partially fill this gap by gathering this information for galaxies in the *Herschel* Reference Survey (HRS; Boselli et al. 2010), a stellar mass and volume-limited sample of nearby systems including galaxies in the Virgo cluster. This provides us with the opportunity of quantifying, for the first time, the effect of the cluster environment on the gas-to-dust ratio of galaxies, and to try to reconcile studies of metals, dust, and cold gas in high-density environments.

Of course, given the limited number statistics of this sample, we can only compare galaxies inside and outside the Virgo cluster, and it is impossible to quantify the effect of environment in smaller groups and pairs. Despite this, it is important to remember that the HRS is currently the largest representative sample of field and cluster galaxies for which estimates of all phases of the ISM are available. For example, samples such as the GALEX Arecibo SDSS Survey (Catinella et al. 2010) do not include information on the dust content of galaxies.

## 2 THE DATA

The HRS is a *K*-band-, volume-limited sample of 322 local galaxies. An extensive description of the sample selection can be found in Boselli et al. (2010), while updated morphologies and distance estimates are presented in Cortese et al. (2012b). For this work, we focus on a subsample of the HRS for which total cold gas (i.e. atomic plus molecular hydrogen), dust and stellar masses are available.

Atomic and molecular gas estimates are taken from Boselli, Cortese & Boquien (2014a). H I masses are derived mainly from single-dish 21 cm flux densities and are available for 315 galaxies in the sample: 263 detected and 52 not detected. For non-detections,  $5\sigma$  upper-limits to the H I masses are calculated assuming a velocity width of  $300 \text{ km s}^{-1}$ . Molecular hydrogen masses have been estimated from CO(1–0) observations. Given the large uncertainty in the CO(1–0) to H<sub>2</sub> conversion factor ( $X_{\text{CO}}$ ), it is important to make sure that our results are independent of the assumptions made on  $X_{\text{CO}}$ . Thus, we investigate both a constant value of  $X_{\text{CO}}$  throughout the sample ( $2.3 \times 10^{20} [\text{cm}^{-2} (\text{K km s}^{-1})^{-1}]$ , typical of Milky Way-like discs) and an *H*-band luminosity dependent conversion factor ( $X_{\text{CO}} = -0.38 \times \log(L_{\text{H}}/L_{\odot}) + 24.23 [\text{cm}^{-2} (\text{K km s}^{-1})^{-1}]$ ) as calibrated in Boselli, Lequeux & Gavazzi (2002). The *H* band is mainly used here as a proxy for metallicity in order to be able to follow the effect of a metallicity-dependent  $X_{\text{CO}}$  without the need of oxygen abundance estimates for all our galaxies. Out of the 225 galaxies observed in CO(1–0), 143 have been detected. For the remaining 82 objects,  $5\sigma$  upper limits have been determined by assuming a CO velocity width equal to the H I width, when available, or to  $300 \text{ km s}^{-1}$  in case of H I non-detections.

Dust masses have been estimated as follows. For the 262 HRS galaxies detected across the entire 8 to  $500 \mu\text{m}$  wavelength range, we use the values presented in Ciesla et al. (2014), which have been obtained by fitting the Draine & Li (2007) dust models to the infrared spectral energy distribution. For the 38 galaxies not detected in neither of the three *Herschel*/SPIRE bands, we estimate  $5\sigma$  upper-limits to their dust masses following the method presented in Cortese et al. (2012a). These are based on the  $350 \mu\text{m}$  flux densities assuming a dust emissivity coefficient ( $\beta$ ) equal to 2. The remaining 22 galaxies, for which a complete dust spectral energy distribution cannot be determined, are excluded from our sample to avoid possible biases in the dust mass estimates. Although the use

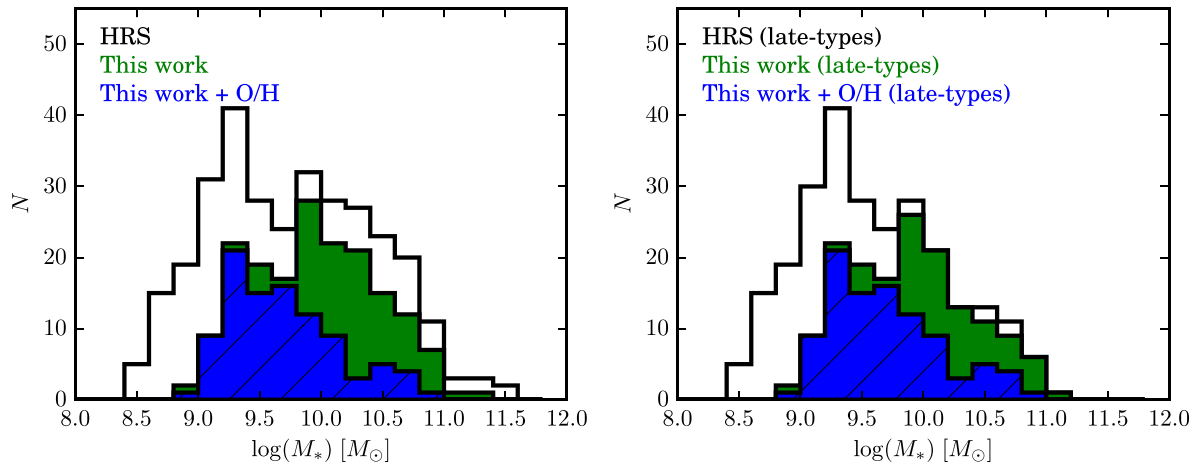


**Figure 1.** Left: the stellar mass distribution for HRS galaxies (empty histogram) and for the subsample used in this work (filled green histogram). The blue hashed histogram shows the stellar mass distribution of galaxies used in this work for which also gas-phase oxygen abundance estimates are available. Right: same as the left-hand panel, but for late-type galaxies (Sa or later types) only.

of the Draine & Li (2007) dust models require a wider wavelength coverage (8–500  $\mu\text{m}$ ) than what needed to fit a single modified blackbody to the *Herschel* SPIRE and PACS bands (100–500  $\mu\text{m}$ ), we note that this requirement does not introduce any significant bias to our sample. Indeed, out of the 22 galaxies detected in at least one *Herschel* band but excluded from our sample, cold gas mass estimates are available for 15 objects, and for only six of these a modified blackbody fit with  $\beta = 2$  (needed to be consistent with the Draine & Li 2007 dust models) is successful in providing a dust mass estimate (see Cortese et al. 2014 for a description of single modified blackbody fits to HRS galaxies).

Finally, stellar mass estimates are taken from Cortese et al. (2012b), which were obtained from the Sloan Digital Sky Survey *g*- and *i*-band magnitudes using the empirical recipes presented in Zibetti, Charlot & Rix (2009).

In order to look for any variations in the  $M_{\text{gas}}/M_{\text{dust}}$  ratio of galaxies across environment, we focus our attention on the subsample of HRS galaxies for which stellar, dust, atomic and molecular gas mass estimates are available, and for which at least one of the three ISM components has been detected. This second condition is crucial for deriving meaningful upper (or lower) limits to the  $M_{\text{gas}}/M_{\text{dust}}$  ratio. Thus, our sample is composed of 176 HRS galaxies. For 122 objects ( $\sim 70$  per cent of our final sample), all three ISM phases have been detected, for 41 galaxies we have detections of both dust and one gas component (35 in  $\text{H I}$  and 6 in  $\text{H}_2$  – we will refer to these galaxies as ‘interval censored data’), whereas for the remaining 13 objects we either detect only dust (5 galaxies) or only gas (8 systems). Thus, the  $M_{\text{gas}}/M_{\text{dust}}$  ratio remains poorly constrained for only  $\sim 7$  per cent of our sample, as for interval censored data we are able to determine both upper and lower limits to the real value.

Our final sample is approximately half of the entire HRS, and it is important to determine whether it is still representative of the entire survey. We investigate this in Fig. 1, where we compare the stellar mass distribution for the entire HRS (empty histogram) with that of the sample used in this paper (filled green histogram). For stellar masses greater than  $\sim 10^{9.2} M_{\odot}$ , our completeness is 70 per cent or higher across all stellar masses, whereas it rapidly decreases for smaller galaxies. This low completeness for dwarf galaxies is mainly due to the lack of CO(1–0) observations (Boselli et al. 2014a). Moreover, our completeness further improves at high

stellar masses, if we consider late-type galaxies only (i.e. Sa or later-types; right-hand panel in Fig. 1). A simple Kolmogorov–Smirnov (KS) test suggests that we cannot reject the null hypothesis that the stellar mass distribution of our sample is drawn from the one of the full HRS above a stellar mass of  $\sim 10^9 M_{\odot}$  at a  $\sim 25$  per cent level, suggesting that our selection criteria have not introduced significant biases.

In Fig. 1, we also show the stellar mass distribution of galaxies in our final sample for which gas-phase oxygen abundances on the Pettini & Pagel (2004) base metallicity calibration can be determined from emission lines (blue hashed histogram; Hughes et al. 2013). The large difference between the blue and the green histograms (96 versus 176 galaxies) highlights the benefits of using the  $M_{\text{gas}}/M_{\text{dust}}$  ratio, instead of gas-phase metallicity, to investigate the enrichment history of galaxies, particularly those with stellar mass greater than  $\sim 10^{10} M_{\odot}$ . Indeed, in this case the KS test rejects the null hypothesis at a  $\sim 0.5$  per cent level.

### 3 THE TOTAL GAS-TO-DUST RATIO ACROSS ENVIRONMENT

We define the total  $M_{\text{gas}}/M_{\text{dust}}$  ratio as  $1.3 \times (M_{\text{H I}} + M_{\text{H}_2})/M_{\text{dust}}$ , where the 1.3 coefficient is included to account for the contribution of Helium. Only if, out of the three ISM components, just one of the two gas phases has been detected, conservative lower limits to the gas-to-dust ratio are defined as  $1.3 \times M_{\text{H I}}/M_{\text{dust}}$  and  $1.3 \times M_{\text{H}_2}/M_{\text{dust}}$ , for  $\text{H I}$ -only or  $\text{H}_2$ -only detections, respectively.

Throughout this paper, we will refer to the gas-to-dust ratio as  $M_{\text{gas}}/M_{\text{dust}}$ , instead of GDR as typically done in the literature. This is to remind the reader that here we investigate total mass ratios, whereas the original definition of GDR (in both observational and theoretical works) is based on the ratio of column densities. Since the distribution of the three ISM components in galaxies is not the same (see also Section 4), the total mass and surface density ratios may differ.

Following Cortese et al. (2012a), we investigate the effect of environment in two complementary ways. First, we divide galaxies according to their Virgo cluster membership (Fig. 2, left-hand panels): i.e. Virgo cluster members (84 galaxies) and galaxies outside Virgo (92 galaxies). Secondly, we use the  $\text{H I}$ -deficiency parameter

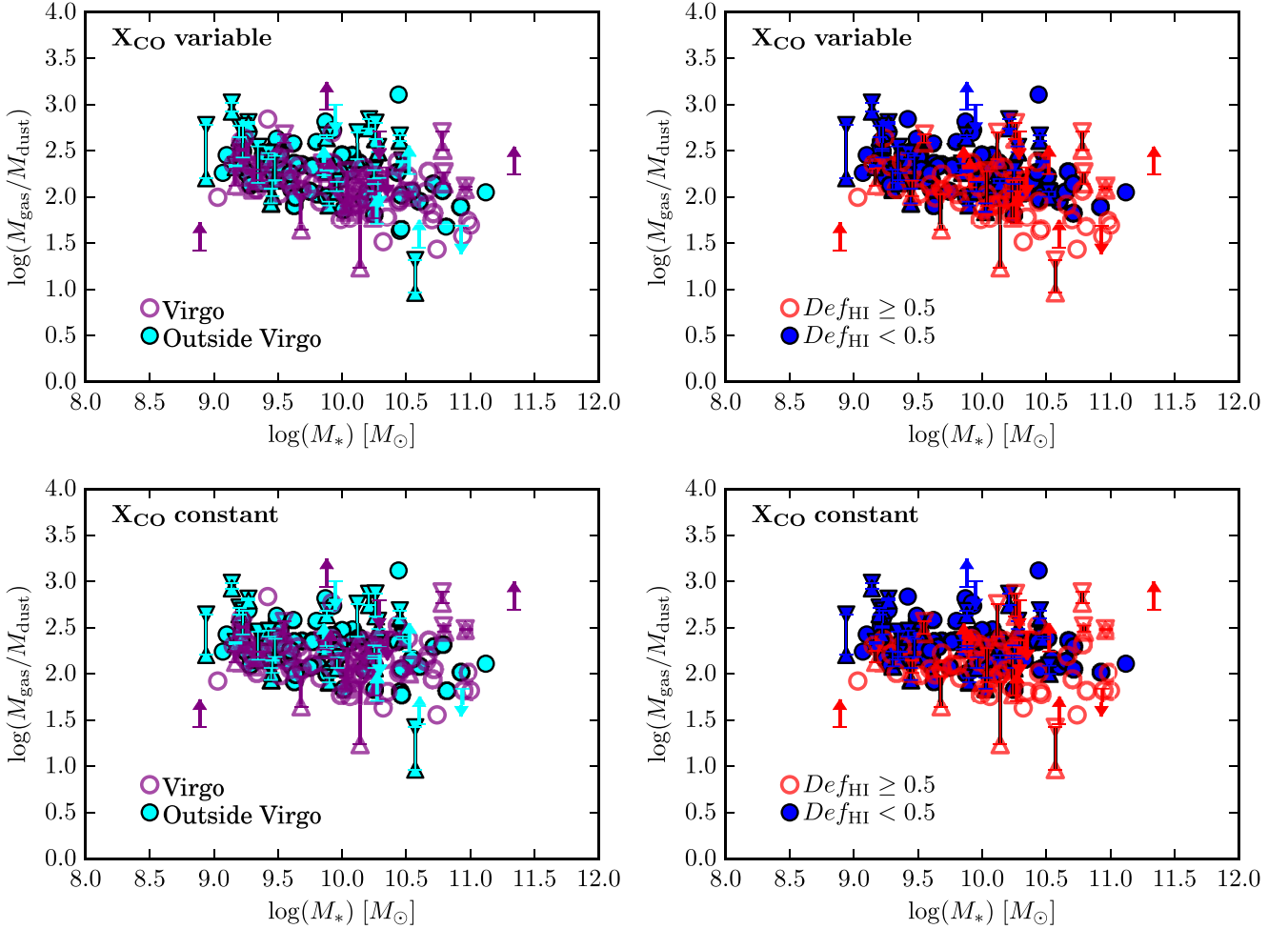


**Figure 2.** The  $M_{\text{gas}}/M_{\text{dust}}-M_*$  relation for galaxies in the HRS. Circles and arrows indicate detections and upper-limits, respectively. Interval censored data (i.e. galaxies for which dust and only one gas phase are detected) are presented as connected triangles, showing the possible range of variation in  $M_{\text{gas}}/M_{\text{dust}}$  obtained by setting the non-detected phase to either zero or its  $5\sigma$  upper limit. The left column shows a comparison between Virgo cluster members (empty purple) and galaxies outside the Virgo cluster (filled cyan), whereas in the right column galaxies are divided according to their H I content, with H I-deficient and H I-normal galaxies as red empty and blue filled symbols, respectively. The top and bottom rows show results obtained for a variable and constant CO-to-H<sub>2</sub> ( $X_{\text{CO}}$ ) conversion factor, respectively.

( $\text{Def}_{\text{H I}}$ ) as an environmental indicator (Fig. 2, right-hand panels).  $\text{Def}_{\text{H I}}$  is defined as the logarithmic difference between the expected H I mass for an isolated galaxy with the same morphological type and optical diameter of the target and the observed value (Haynes & Giovanelli 1984), and it is generally adopted to identify environmentally perturbed systems. We use a value of  $\text{Def}_{\text{H I}} = 0.5$  (i.e. 70 per cent less H I than expected) to discriminate between H I-stripped galaxies (69 galaxies) and ‘unperturbed’ systems (107 galaxies).<sup>1</sup> The difference between the top and bottom rows is simply due to the different CO to H<sub>2</sub> conversion factor used:  $X_{\text{CO}}$  varying with  $H$ -band luminosity (top), or  $X_{\text{CO}}$  constant (bottom).

In all panels, circles show the 122 galaxies for which all the three ISM phases are detected, and arrows indicate the 13 objects for which either only gas or dust are detected. The remaining 41 galaxies, for which dust and one gas phase are detected, are presented as

connected triangles, where the two triangles correspond to the upper and lower limit to the  $M_{\text{gas}}/M_{\text{dust}}$  obtained by setting the undetected gas phase to its  $5\sigma$  upper limit or to zero, respectively.

As recently shown by Rémy-Ruyer et al. (2014), we confirm that the  $M_{\text{gas}}/M_{\text{dust}}$  ratio monotonically decreases with stellar mass regardless of environment. The slope of the relation depends on the value of  $X_{\text{CO}}$  used but, even for a constant conversion factor, we see an average variation in the  $M_{\text{gas}}/M_{\text{dust}}$  ratio of  $\sim 0.2$  dex when moving from less ( $\sim 10^{9.4} M_{\odot}$ ) to more massive ( $\sim 10^{10.7} M_{\odot}$ ) systems, with a scatter of 0.25–0.3 dex.

In order to quantify the effect of environment on the  $M_{\text{gas}}/M_{\text{dust}}-M_*$  relation in Fig. 3, we present the best-linear fits for each subsample as well as the median and their bootstrapped errors per bin of stellar mass (see Table 1). We fix interval censored data to their upper limits and left/right censored data to their upper/lower limits, but our conclusions are independent on how interval censored data are treated.

Regardless the choice of  $X_{\text{CO}}$ , when galaxies are divided according to their cluster membership, an effect of the environment is evident only in the lower stellar mass bin, with cluster galaxies having  $\sim 0.15$  dex lower  $M_{\text{gas}}/M_{\text{dust}}$  ratio than field systems. Indeed, at

<sup>1</sup> It is important to remember that, although the vast majority of H I-deficient galaxies (54 galaxies) are either Virgo member or lie in its infalling regions, some of them are found in groups (see also Catinella et al. 2013). However, our conclusions are unchanged if we remove from our sample H I-deficient galaxies outside Virgo.

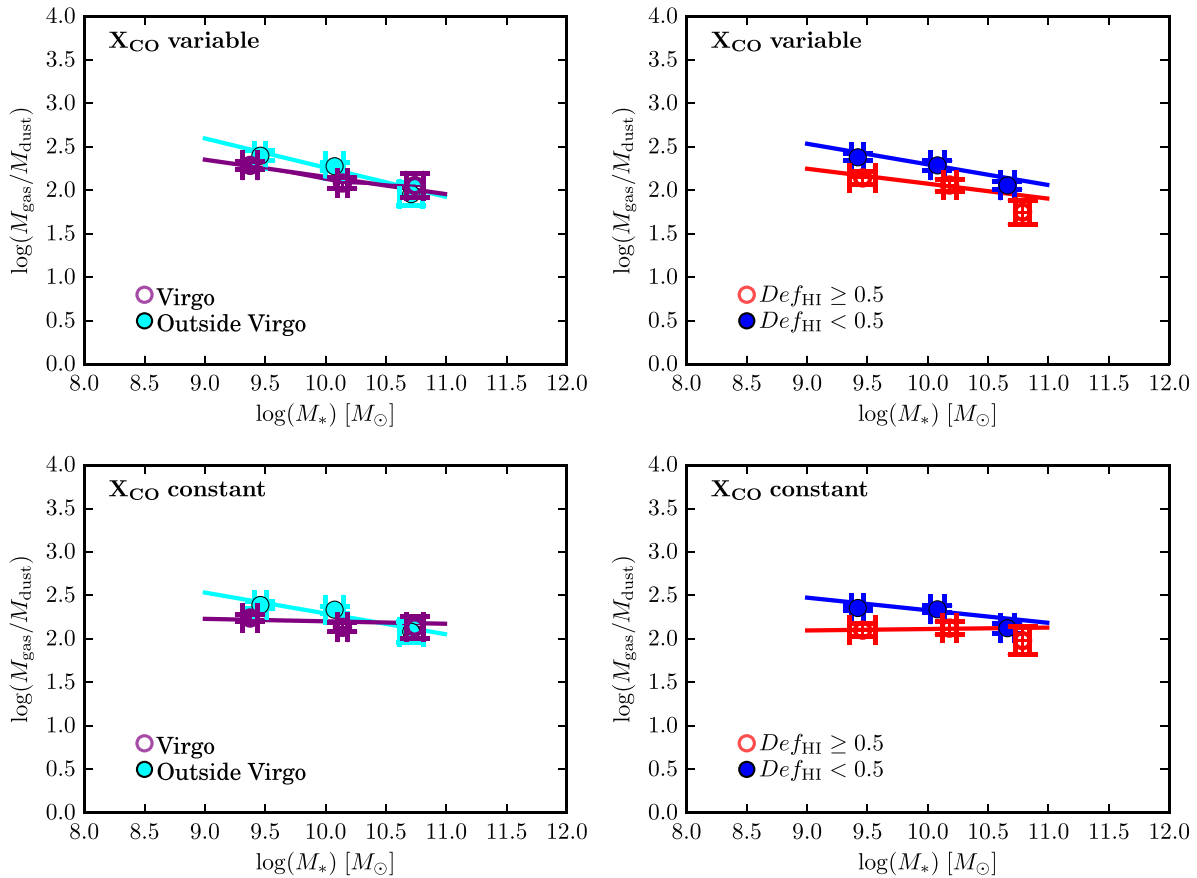


**Figure 3.** The  $M_{\text{gas}}/M_{\text{dust}}-M_*$  relation for galaxies in the HRS. Points show median values per bin of stellar mass, whereas lines show the best linear fits to the data. Errors on the median are obtained using 1000 bootstrap re-samplings of the data in each bin (see Table 1). Panels and colours are as in Fig. 2.

**Table 1.** The median  $M_{\text{gas}}/M_{\text{dust}}$  ratio per bin of  $M_*$  for HRS galaxies outside Virgo, Virgo cluster members, H I-normal, and H I-deficient systems. Errors on the median are obtained using 1000 bootstrap re-samplings of the data in each bin.

$\log(M_*/M_\odot)^a$	$\log(M_{\text{gas}}/M_{\text{dust}})$ $X_{\text{CO}} \text{ constant}$	$\log(M_{\text{gas}}/M_{\text{dust}})$ $X_{\text{CO}} \text{ variable}$	$N_{\text{gal}}$
Outside Virgo			
9.46	$2.39 \pm 0.04$	$2.40 \pm 0.06$	37
10.08	$2.34 \pm 0.04$	$2.28 \pm 0.04$	44
10.71	$2.08 \pm 0.12$	$1.96 \pm 0.14$	11
Virgo members			
9.38	$2.24 \pm 0.04$	$2.29 \pm 0.04$	32
10.14	$2.13 \pm 0.05$	$2.09 \pm 0.06$	37
10.74	$2.14 \pm 0.13$	$2.06 \pm 0.14$	15
H I-normal ( $\text{Def}_{\text{H I}} < 0.5$ )			
9.42	$2.36 \pm 0.03$	$2.38 \pm 0.04$	52
10.08	$2.34 \pm 0.04$	$2.29 \pm 0.05$	45
10.66	$2.12 \pm 0.06$	$2.06 \pm 0.04$	10
H I-deficient ( $\text{Def}_{\text{H I}} \geq 0.5$ )			
9.46	$2.10 \pm 0.08$	$2.14 \pm 0.08$	17
10.18	$2.12 \pm 0.07$	$2.06 \pm 0.07$	36
10.79	$1.98 \pm 0.16$	$1.75 \pm 0.14$	16

*Note.* <sup>a</sup>Stellar mass bins are identical for each subsample: i.e.  $\log(M_*/M_\odot) < 9.8$ ,  $9.8 \leq \log(M_*/M_\odot) \leq 10.5$  and  $\log(M_*/M_\odot) > 10.5$ .

higher stellar masses, the difference in the average  $M_{\text{gas}}/M_{\text{dust}}$  ratio for the two samples is within the errors. This is in line with previous results based on the mass–metallicity relations of cluster galaxies (e.g. Mouhcine et al. 2007; Ellison et al. 2009; Petropoulou et al. 2012; Hughes et al. 2013), and in particular with the recent work by Petropoulou et al. (2012), who found that the effect of the cluster environment on the gas-phase metallicity becomes significant only for  $M_* < 10^{9.5} M_\odot$ . When galaxies are separated according to their H I content, the effect of environment becomes slightly more significant ( $\sim 2\sigma$ – $2.5\sigma$  level on average) with H I-deficient galaxies having an  $M_{\text{gas}}/M_{\text{dust}}$  ratio  $\sim 0.2$ – $0.3$  dex lower than H I-normal systems, at all stellar masses, independently of the choice of  $X_{\text{CO}}$ .

These results show that the effect of the environment on the  $M_{\text{gas}}/M_{\text{dust}}$  is rather limited and becomes evident only if we pre-select galaxies that have already been affected by the environment based on their H I deficiency measurement. This is in line with the lack of strong environmental dependence observed in the stellar mass versus gas-phase metallicity relation (Hughes et al. 2013). As extensively discussed in Cortese et al. (2012a), this is simply due to the fact that cluster membership does not imply that environment has already been able to play a significant role.

In order to further investigate why the  $M_{\text{gas}}/M_{\text{dust}}$  ratio shows at most a factor of 2 variation with environment despite the fact that the H I reservoir of H I-deficient galaxies has been depleted by more than a factor of 3, we now consider the gas-to-dust ratio for the H I and H<sub>2</sub> phases, separately. In Fig. 4, which represents the main result of this work, we plot the  $M_{\text{H I}}/M_{\text{dust}}$  (left) and  $M_{\text{H}_2}/M_{\text{dust}}$



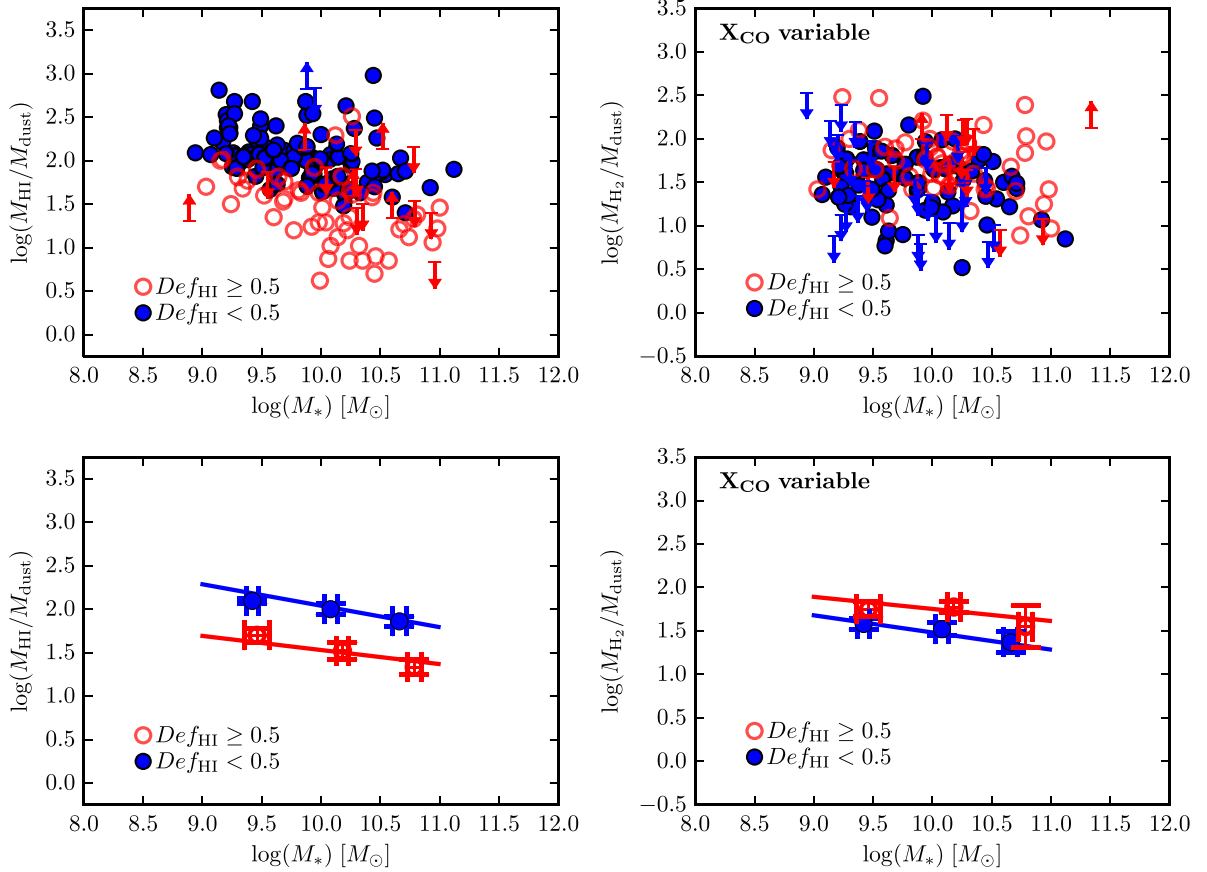


**Figure 4.** The  $M_{\text{HI}}/M_{\text{dust}}-M_*$  (left) and  $M_{\text{H}_2}/M_{\text{dust}}-M_*$  (right) relations for H I-normal (filled blue) and H I-deficient (empty red) HRS galaxies. Individual galaxies are shown in the upper panels, with circles and arrows indicating detections and upper/lower limits, respectively. Averages per bin of stellar mass and best linear fits are shown in the bottom panels.

**Table 2.** The median  $M_{\text{HI}}/M_{\text{dust}}-M_*$  and  $M_{\text{H}_2}/M_{\text{dust}}-M_*$  relations for H I-normal and H I-deficient galaxies. Errors on the median are obtained using 1000 bootstrap re-samplings of the data in each bin.

$\log(M_*/M_\odot)$	$\log(M_{\text{HI}}/M_{\text{dust}})$	$\log(M_{\text{H}_2}/M_{\text{dust}})$ $X_{\text{CO}}$ constant	$\log(M_{\text{H}_2}/M_{\text{dust}})$ $X_{\text{CO}}$ variable	$N_{\text{gal}}$
H I-normal ( $\text{Def}_{\text{HI}} < 0.5$ )				
9.42	$2.10 \pm 0.03$	$1.47 \pm 0.09$	$1.58 \pm 0.06$	52
10.08	$2.00 \pm 0.06$	$1.73 \pm 0.10$	$1.52 \pm 0.08$	45
10.66	$1.86 \pm 0.05$	$1.68 \pm 0.11$	$1.37 \pm 0.13$	10
H I-deficient ( $\text{Def}_{\text{HI}} \geq 0.5$ )				
9.46	$1.70 \pm 0.08$	$1.70 \pm 0.11$	$1.75 \pm 0.09$	17
10.18	$1.52 \pm 0.10$	$1.84 \pm 0.09$	$1.78 \pm 0.06$	36
10.79	$1.33 \pm 0.07$	$1.91 \pm 0.22$	$1.55 \pm 0.25$	16

(right) ratios as a function of stellar mass for our sample. Individual galaxies are shown in the top row, while median per bin of stellar mass and best linear fits are presented in the bottom row. We only focus on the comparison between H I-deficient (red) and H I-normal (blue) galaxies, as this is the case for which the effect of environment is stronger. We also show the case of variable  $X_{\text{CO}}$  factor only, but the results for a constant value of  $X_{\text{CO}}$  are included in Table 2.

The difference between H I-poor and H I-normal galaxies is larger once the atomic and molecular components are considered separately. In particular, the  $M_{\text{HI}}/M_{\text{dust}}$  ratio is  $\sim 0.5$  dex lower in H I-deficient galaxies (see Table 2). As already discussed in Cortese et al. (2012a), this is consistent with the idea that the H I, extending

to larger radii than the dust, is more strongly affected by the environment. The improvement with respect to our previous work is simply in the use of more accurate H I and dust mass estimates. Remarkably, the  $M_{\text{H}_2}/M_{\text{dust}}$  ratio shows the *opposite trend* (see Fig. 4 left), with H I-deficient systems having systematically higher  $M_{\text{H}_2}/M_{\text{dust}}$  ratios than H I-normal galaxies at fixed stellar mass ( $\sim 0.2$  dex). Moreover, both the  $M_{\text{HI}}/M_{\text{dust}}-M_*$  and  $M_{\text{H}_2}/M_{\text{dust}}-M_*$  relations have a scatter slightly larger ( $\sim 0.35$  dex) than the  $M_{\text{gas}}/M_{\text{dust}}-M_*$  trend ( $\sim 0.25$ – $0.3$  dex). As shown in Table 2, the slope of the  $M_{\text{H}_2}/M_{\text{dust}}-M_*$  depends on the choice of  $X_{\text{CO}}$  (i.e. decreasing/increasing with stellar mass for  $X_{\text{CO}}$  variable/constant), as expected if the  $M_{\text{H}_2}/M_{\text{dust}}$  ratio is roughly constant with metallicity. Conversely, the

difference between H I-poor and H I-normal systems does not depend on  $X_{\text{CO}}$ .

Admittedly, while the change in the  $M_{\text{H I}}/M_{\text{dust}}$  ratio has a high statistical significance, it becomes marginal (i.e.  $\sim 1\sigma$ – $1.5\sigma$  level on average) for the  $M_{\text{H}_2}/M_{\text{dust}}$  ratio. This is due to the larger error in the CO measurements and aperture corrections, as well as the higher fraction of non-detections.

We can safely exclude that our findings are an artefact due to the aperture correction applied to the CO data (see Boselli et al. 2014a). Indeed, the typical fractional coverage of the CO observations is roughly the same for both classes of galaxies, and the same result is obtained if we consider the uncorrected data.

By combining the results presented in the two panels of Fig. 4, it is clear why the  $M_{\text{gas}}/M_{\text{dust}}$  ratio varies so little with environment: the reduction in  $M_{\text{H I}}/M_{\text{dust}}$  ratio seems partly balanced by an increase in  $M_{\text{H}_2}/M_{\text{dust}}$  for cluster galaxies. In other words, the absence of a large variation in the  $M_{\text{gas}}/M_{\text{dust}}$  ratio (and similarly of gas-phase metallicity) as function of environment does not automatically imply that the environment is not able to affect the different phases of the ISM. On the contrary, each phase is removed in such a way that the net effect on the  $M_{\text{gas}}/M_{\text{dust}}$  ratio is relatively small.

#### 4 DIFFERENTIAL STRIPPING OF THE ISM

A natural scenario that could explain the results presented in Fig. 4 is stripping by ram pressure. The hydrodynamic pressure of the intracluster medium on galaxies removes primarily the ISM in the outer-parts of the disc, which are generally H I-dominated compared to the inner effective radius where most of the neutral hydrogen is condensed into molecules. Thus, if environment is more efficient in the outskirts of galaxies, the net effect on the total gas and dust reservoirs is simply related to how extended their distributions are. In other words, in case of ram pressure, the evidence for differential stripping shown in the previous section may be simply a consequence of the different scalelengths of the H I, H<sub>2</sub>, and dust discs.

We test this hypothesis in two different, complementary, ways. In the first one, we use an analytical approximation to show how we can reproduce our findings with simple assumptions on the distribution of gas and dust in the disc. In the second one, we take advantage of the Bekki (2013, 2014a,b) model to follow the effect of ram pressure on the various components of the ISM in a self-consistent way.

##### 4.1 Analytical approximation

The basic assumption behind our analytical approach is that all three components of the ISM are fully stripped by ram pressure up to the same stripping radius. Thus, to determine how a galaxy would move in Figs 2 and 4, we simply need to estimate how much mass is left within the stripping radius.

For the H I distribution, we assume the functional form presented in Hewitt, Haynes & Giovanelli (1983) by studying a sample of 52 nearby galaxies mapped with the Arecibo telescope:

$$\Sigma_{\text{H I}}(r) = 3e^{-\frac{r^2}{R_0^2}} - 1.8e^{-\frac{r^2}{0.23R_0^2}} \quad (1)$$

and fix  $R_0$  equal to the optical radius ( $R_{\text{opt}}$ ). The double Gaussian shape is used to reproduce the central depression in the H I surface density profile, where most of the gas has already condensed into molecules, as typically observed in late-type galaxies (Leroy et al. 2008).

Conversely, we consider an exponential surface density distribution for both dust and H<sub>2</sub>

$$\Sigma(r) = \Sigma(0)e^{-r/R_d} \quad (2)$$

with  $R_d(\text{dust}) = R_{\text{opt}}/3.2$  (i.e. the dust follows the stellar mass distribution; Muñoz-Mateos et al. 2009; Smith et al., submitted) and  $R_d(\text{H}_2) = 0.2R_{\text{opt}}$  (Schruba et al. 2011).

In the ideal case where all the material outside the stripping radius ( $R_{\text{strip}}$ ) is removed by ram pressure, we can determine the reduction in the mass of each component after stripping as

$$\frac{M_{\text{after}}}{M_{\text{before}}} = \frac{\int_0^{R_{\text{strip}}} 2\pi r \Sigma(r) dr}{\int_0^\infty 2\pi r \Sigma(r) dr}. \quad (3)$$

For the atomic hydrogen this gives

$$\frac{M_{\text{after}}}{M_{\text{before}}} = 1 - 1.16e^{-\frac{R_{\text{strip}}^2}{R_0^2}} + 0.16e^{-\frac{R_{\text{strip}}^2}{0.23R_0^2}}, \quad (4)$$

whereas for dust and H<sub>2</sub>

$$\frac{M_{\text{after}}}{M_{\text{before}}} = 1 - \left(1 + \frac{R_{\text{strip}}}{R_d}\right) e^{-\frac{R_{\text{strip}}}{R_d}}. \quad (5)$$

Taking advantage of equations (4) and (5), we can now determine how a galaxy will shift in Figs 2 and 4, depending on the size of the stripping radius. We assume the best-fitting linear relation for H I-normal galaxies as the reference in case of unperturbed systems and consider values of  $R_{\text{strip}}$  in the range  $0.3$ – $2R_{\text{opt}}$  (0.2 wide steps). We also consider an average molecular-to-atomic fraction of  $\sim 27$  per cent, i.e. the average value for our H I-normal galaxies.

The expected shifts in the  $M_{\text{gas}}/M_{\text{dust}}$ ,  $M_{\text{H I}}/M_{\text{dust}}$ , and  $M_{\text{H}_2}/M_{\text{dust}}$  ratios for different stripping radii are presented in the top panel of Fig. 5. It emerges that, under the simple assumptions discussed above, we can quantitatively reproduce the difference between H I-deficient and H I-normal galaxies in  $M_{\text{gas}}/M_{\text{dust}}$ ,  $M_{\text{H I}}/M_{\text{dust}}$ , and  $M_{\text{H}_2}/M_{\text{dust}}$  ratios simultaneously, by assuming a typical stripping radius for H I-deficient galaxies of  $\sim 0.5R_{\text{opt}}$ . For the H I component, this degree of stripping is in line with what is observed in H I-deficient galaxies in Virgo. Indeed, by taking advantage of the data presented in (Chung et al. 2009, see also fig. 2 in Cortese et al. 2010a), it is easy to show that  $\text{Def}_{\text{H I}} > 0.5$  implies  $R_{\text{strip}} < 0.9R_{\text{opt}}$ . Interestingly, this simple model is also able to quantitatively reproduce the correlation between H I and H<sub>2</sub> deficiency observed by Boselli et al. (2014b), with H<sub>2</sub> deficiencies above  $\sim 0.3$  only when  $\text{Def}_{\text{H I}} > 1$ .

##### 4.2 Bekki's model

Although physically motivated, the analytical approximation described above is rather empirical and not self-consistent. In particular, it does not take into account the possible small increase of star formation due to gas compression by ram pressure, and it naively assumes that ram pressure equally affects all three ISM components outside the stripping radius, which may not always be true (Pappalardo et al. 2012). Thus, in this section we compare our findings with the predictions of the model developed by Bekki (2013, 2014a,b). Although this model is not set in a cosmological framework, it is the only model currently available where the evolution of the three different phases, and the effect of environment, is followed in a self-consistent way. Cosmological simulations are only now starting to include dust formation models (McKinnon, Torrey & Vogelsberger 2016), as so far they have just assumed a linear correlation between gas-to-dust ratio and metallicity.

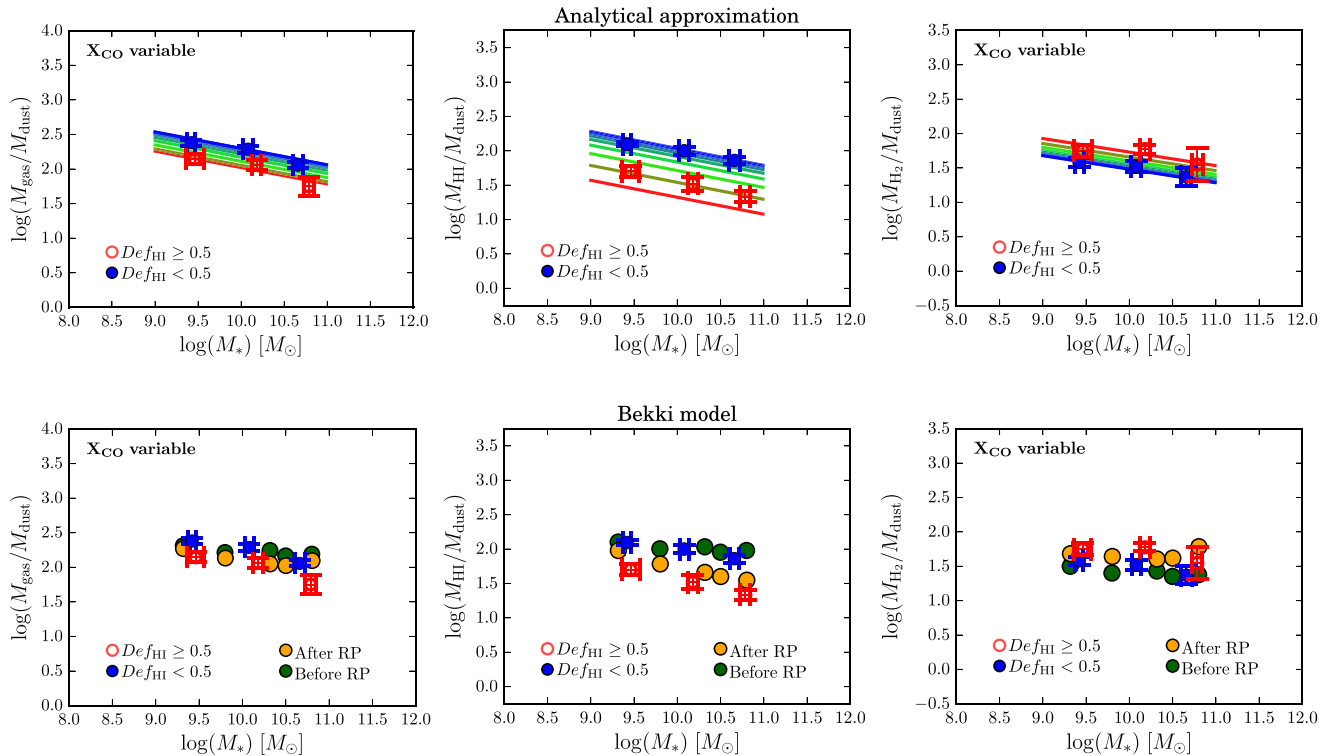


**Figure 5.** The average  $M_{\text{gas}}/M_{\text{dust}}$  (left),  $M_{\text{HI}}/M_{\text{dust}}$  (centre) and  $M_{\text{H}_2}/M_{\text{dust}}$  (right) ratios per bin of  $M_*$  for H I-normal (filled blue) and H I-deficient (empty red) galaxies, reproduced from Figs 3 and 4. The top panel shows the predictions for our simple analytical model where all ISM components are removed outside the stripping radius. Coloured lines show stripping radii decreasing from  $2 \times R_{\text{opt}}$  (i.e. no stripping, blue) to  $0.3 \times R_{\text{opt}}$  (red), in  $0.2 \times R_{\text{opt}}$  steps. The bottom panels show the predictions of Bekki (2013, 2014a,b) models. Green and yellow circles show the predictions before and after ram-pressure stripping.

This model allows us to investigate spatial and temporal variations of gas and dust components (carbon and silicate dust) in disc galaxies with different masses and Hubble types. The code adopts the smoothed-particle hydrodynamics method to follow the time evolution of gas dynamics in galaxies.

An extensive description of the model is provided in Bekki (2013, 2014a,b), here we briefly summarize its main features. A disc galaxy is modelled as a fully self-gravitating system composed of dark matter halo, stellar and gaseous discs, and stellar bulge. Although we investigated numerous models, we show only five representative models with dark matter haloes of  $10, 5, 3.3, 1,$  and  $0.33 \times 10^{11} M_{\odot}$  and disc stellar masses of  $5.4, 2.7, 1.8, 0.54,$  and  $0.18 \times 10^{10} M_{\odot}$ . We will explore other models, and their implications on dust and gas evolution in cluster environments in a future paper.

The gas disc is assumed to have an exponential profile with its size initially twice the stellar disc and the gas mass fraction is set to be 0.18. The initial gaseous metallicities of disc galaxies are calibrated on the mass–metallicity relation, spanning the range  $-0.11 < [\text{Fe}/\text{H}] < 0.34$ , with a negative radial metallicity gradient of  $-0.04 \text{ dex kpc}^{-1}$ .

Dust formation from ejecta of AGB stars and supernovae is self-consistently implemented. The initial dust-to-metal ratio is set to be 0.4 (as observed for the Milky Way), and the initial  $M_{\text{gas}}/M_{\text{dust}}$  ratio gradient follows the metallicity gradient. In order to avoid further introduction of free parameters on dust, we do not include the dust growth and destruction for  $\sim 1$  Gyr evolution of disc galaxies under ram pressure of intracluster medium in this study.

The mass of cold gas present in the molecular phase is determined by the balance between  $\text{H}_2$  condensation on dust grains from atomic

gas and photodissociation by the far-ultraviolet radiation field (see equation 16 in Bekki 2013). For a given gas density, total dust-to-gas-ratio, and intensity of the interstellar radiation field, the  $\text{H}_2$  mass fraction associated to each particles, and thus the galaxy  $\text{H}_2$  profile, can be determined.

The strength of ram-pressure force on the disc is time-dependent and modelled in the same way as in Bekki (2014a). We consider a Virgo-like cluster with a total mass of  $10^{14} M_{\odot}$  and a temperature of the intra-cluster medium (ICM)  $T_{\text{ICM}} = 2.6 \times 10^7 \text{ K}$ , in line with the observed values for the Virgo A cloud (Bohringer et al. 1994; Schindler, Binggeli & Böhringer 1999). The total ICM mass is 15 per cent of the dark matter mass of the cluster and both dark matter and ICM are assumed to follow a Navarro, Frenk & White (1997) profile. In order to show the effects of ram pressure on the ISM we choose the orbits of disc galaxies for which stripping can be efficient, but part of the gas is left within the disc after the first passage (otherwise no  $M_{\text{gas}}/M_{\text{dust}}$  ratio can be estimated). The initial velocity of the galaxy is  $617 \text{ km s}^{-1}$ , but this increases to  $1246 \text{ km s}^{-1}$  at the pericentre, which is set to 30 kpc from the cluster centre.

The predictions of this model are shown in the bottom row of Fig. 5. Green and yellow circles illustrate the results before and after (1 Gyr from the pericentre) ram-pressure stripping. Even once the balance between H I,  $\text{H}_2$ , and dust, as well as the effect of the environment, are modelled in a self-consistent way we reproduce the opposite trends observed in the  $M_{\text{HI}}/M_{\text{dust}}$  and  $M_{\text{H}_2}/M_{\text{dust}}$  ratios. While the quantitative agreement is quite good for the  $M_{\text{gas}}/M_{\text{dust}}$  and  $M_{\text{H}_2}/M_{\text{dust}}$  ratios, the model seems to slightly underestimate the stripping of H I especially in low-mass galaxies. However, this



is likely simply due to the particular choice of orbits assumed here. We stress that the goal of this exercise is to demonstrate that the differential stripping scenario is consistent with our data, not to determine which set of model parameters best fits our observations. There are many assumptions and free variables in the modelling that could be tweaked in order to perfectly match our observations, but looking for an exact fit is beyond the goal of this work.

To conclude, both the theoretical approaches presented here confirm that the changes in the  $M_{\text{gas}}/M_{\text{dust}}$  ratios observed when moving from H I-normal to H I-deficient galaxies are consistent with simple outside-in stripping of the ISM.

Of course, at this stage we cannot exclude that more than one environmental mechanism is responsible for the trends presented in this paper (as a small fraction of our H I-deficient galaxies are in groups). However, all the observational evidence collected so far suggests that stripping by a hydrodynamical mechanism is the main factor to explain the bulk of our H I-deficient population.

## 5 SUMMARY AND CONCLUSION

In this work, we have performed the largest investigation on the effect of environment on the  $M_{\text{gas}}/M_{\text{dust}}$  ratio of nearby galaxies. We have provided evidence for significant reduction in the dust, atomic and molecular hydrogen reservoirs of cluster galaxies, once compared with field systems of the same stellar mass. This ISM removal results in a systematic decrease in the  $M_{\text{H I}}/M_{\text{dust}}$  ratio and increase in the  $M_{\text{H}_2}/M_{\text{dust}}$  ratio for gas-poor systems. However, once both atomic and molecular hydrogen are combined, the net effect of the environment is reduced and, at fixed stellar mass, the  $M_{\text{gas}}/M_{\text{dust}}$  ratio varies by  $\sim 0.2$  dex at most from low- to high-density environments.

Our results do reconcile the clear evidence for gas and dust stripping in clusters, with the absence of any strong environmental trends observed in the stellar mass versus metallicity relation. Indeed, given the tight link between  $M_{\text{gas}}/M_{\text{dust}}$  ratio and gas-phase metallicity (e.g. Burstein & Heiles 1982; Issa et al. 1990; Rémy-Ruyer et al. 2014) observed also in our sample (Fig. 6, top panel), it is natural to see how the tiny change in the oxygen abundance of galaxies (at fixed stellar mass) with environment does not automatically imply that the environment has no effect on the metal content of galaxies. This is particularly true when galaxies are simply divided according to their cluster membership. On the contrary, both metals and hydrogen are affected, but in such a way that their ratio remains nearly constant.

We have shown that the observed variations of  $M_{\text{gas}}/M_{\text{dust}}$ ,  $M_{\text{H I}}/M_{\text{dust}}$ , and  $M_{\text{H}_2}/M_{\text{dust}}$  ratios with environment are consistent with what expected if a hydrodynamical mechanism such as ram-pressure stripping is the main responsible for the removal of the ISM from the disc. In particular, we have highlighted how our findings can be simply understood as a consequence of the different spatial distribution of atomic, molecular hydrogen, and dust across a galaxy: i.e. with molecular hydrogen being more centrally concentrated than dust, and dust more concentrated than H I. Although several previous works have found evidence of differential stripping in cluster galaxies (e.g. Kenney & Young 1986; Vollmer et al. 2009; Tonnesen & Bryan 2010; Cortese et al. 2010a, 2012a; di Serego Alighieri et al. 2013; Boselli et al. 2014b; Kenney et al. 2015), this is the first time that the strengths of this effect is quantified for a large statistical sample and for all three phases of the ISM simultaneously. This work, combined with our previous studies of the HRS (Cortese & Hughes 2009; Hughes & Cortese 2009; Cortese et al. 2011, 2012a; Hughes et al. 2013; Boselli et al. 2014b), allows us to

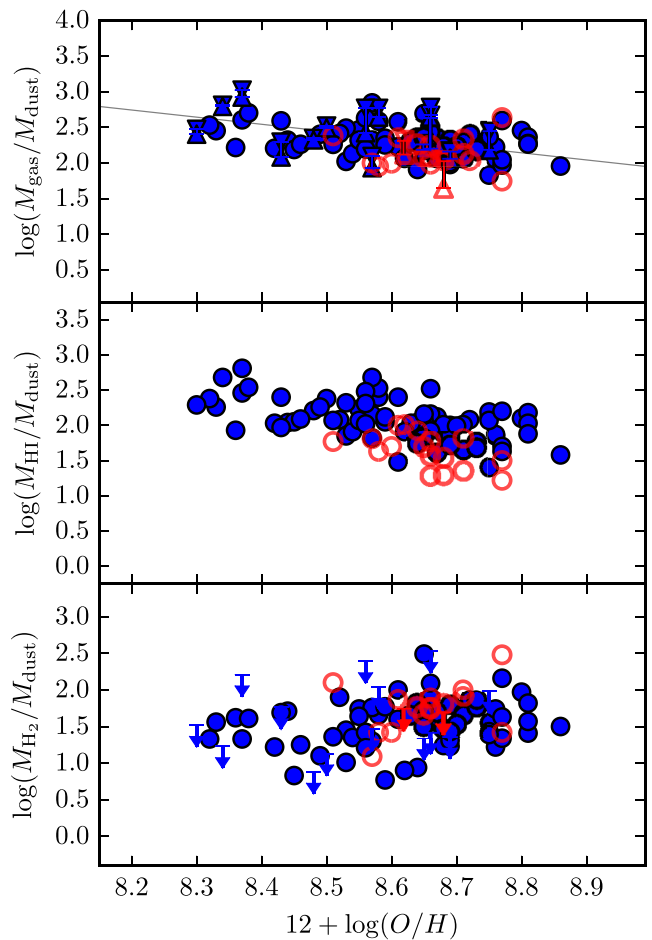


**Figure 6.** The  $M_{\text{gas}}/M_{\text{dust}}$  (top),  $M_{\text{H I}}/M_{\text{dust}}$  (middle), and  $M_{\text{H}_2}/M_{\text{dust}}$  ratios a function of gas-phase metallicities on the PP04 O3N2 base calibration. Symbols are as in the right column of Fig. 2. Note that this plot includes only the subsample of galaxies for which oxygen abundances are available (blue histogram in Fig. 1). The grey solid line in the top panel shows the case  $M_{\text{gas}}/M_{\text{dust}} \propto O/H$ .

complete the analysis of the effect of Virgo cluster environment on the different steps of the star formation cycle of galaxies, confirming that direct stripping of ISM from the disc (e.g. ram pressure) is the main mechanism affecting the star formation cycle of cluster galaxies at the present epoch (see also Boselli et al. 2014c).

Finally, it is worth noting the possible implications of our results for the use of dust continuum emission as a proxy for cold gas content (Eales et al. 2010, 2012; Groves et al. 2015), a technique that is becoming more and more common in high-redshift studies (Magdis et al. 2012; Scoville et al. 2014). The small, but significant (i.e. comparable to the scatter of the relation) variation of the  $M_{\text{gas}}/M_{\text{dust}}$  ratio with environment might suggest that the total dust mass does not always represent an ideal proxy for the total cold hydrogen content of environmentally perturbed galaxies. More importantly, the larger differences between H I-deficient and H I-normal galaxies observed for the  $M_{\text{H I}}/M_{\text{dust}}$  and  $M_{\text{H}_2}/M_{\text{dust}}$  ratios (as well as the larger intrinsic scatter in the relations) show that, at fixed stellar mass, dust emission cannot be easily used to quantify the amount of hydrogen present in either molecular or atomic phase, as the three phases of the ISM are distributed differently across the disc. This is particularly important considering the fact that, when moving from  $z = 0$  to  $z \sim 1$ , the H I/H<sub>2</sub> ratio is expected to decrease significantly,

the gas reservoirs in galaxies at  $z \sim 1$  are thought to be mainly in the molecular phase (Lagos et al. 2011; Popping, Somerville & Trager 2014), and the physical conditions, as well as distribution, of the ISM are remarkably different from those of nearby discs.

However, the above argument does not take into account that the calibration of the dust continuum emission as a gas tracer is generally based on the  $M_{\text{gas}}/M_{\text{dust}}\text{-O/H}$  relation and not on the  $M_{\text{gas}}/M_{\text{dust}}\text{-}M_*$  relation. Since stripping is able to affect the amount of metals in the ISM, but should not change significantly the stellar mass of galaxies, it is possible that the effect of the environment on a  $M_{\text{gas}}/M_{\text{dust}}\text{-O/H}$  diagram would be less strong. Unfortunately, as discussed in Section 2, for nearly half of our sample gas-phase metallicities cannot be estimated, making this kind of test unreliable. Despite this, for completeness we show in Fig. 6 the  $M_{\text{gas}}/M_{\text{dust}}$  (top),  $M_{\text{H I}}/M_{\text{dust}}$  (middle) and  $M_{\text{H}_2}/M_{\text{dust}}$  (bottom) ratios as a function of gas-phase metallicities (taken from Hughes et al. 2013) for H I-normal and H I-deficient galaxies. Given the limited number of gas-poor galaxies available in this sample, we cannot draw firm conclusions, but it is interesting to note that a difference in the  $M_{\text{H}_2}/M_{\text{dust}}$  and  $M_{\text{H I}}/M_{\text{dust}}$  of H I-normal and H I-deficient galaxies is still present. Moreover, it appears that the anti-correlation between  $M_{\text{gas}}/M_{\text{dust}}$  and O/H is primarily driven by the atomic gas phase, whereas very little dependence on metallicity is observed in case of the  $M_{\text{H}_2}/M_{\text{dust}}$ .

We can thus conclude that, until the relation between gas-to-dust ratio and environment is directly investigated in high-redshift galaxies, it remains unclear whether or not the relations between dust and cold gas calibrated on local galaxies provide us with an unbiased view of the gas cycle in galaxies at higher redshifts.

## ACKNOWLEDGEMENTS

We thank the referee for a constructive report which helped improving the quality of this manuscript.

LC and BC acknowledge support under the Australian Research Council Discovery Programme funding schemes (FT120100660, DP130100664, DP150101734). MB acknowledges funding by the FIC-R Fund, allocated to the project 30321072.

LC thanks V. Leboutteiller and J. Fernandez-Ontiveros for comments on this manuscript.

We thank all the people involved in the construction and the launch of *Herschel*. PACS has been developed by a consortium of institutes led by MPE (Germany) and including UVIE (Austria); KU Leuven, CSL, IMEC (Belgium); CEA, LAM (France); MPIA (Germany); INAF-IFSI/OAA/OAP/OAT, LENS, SISSA (Italy); IAC (Spain). This development has been supported by the funding agencies BMVIT (Austria), ESA-PRODEX (Belgium), CEA/CNES (France), DLR (Germany), ASI/INAF (Italy), and CICYT/MCYT (Spain). SPIRE has been developed by a consortium of institutes led by Cardiff University (UK) and including Univ. Lethbridge (Canada); NAOC (China); CEA, LAM (France); IFSI, Univ. Padua (Italy); IAC (Spain); Stockholm Observatory (Sweden); Imperial College London, RAL, UCL-MSSL, UKATC, Univ. Sussex (UK); and Caltech, JPL, NHSC, Univ. Colorado (USA). This development has been supported by national funding agencies: CSA (Canada); NAOC (China); CEA, CNES, CNRS (France); ASI (Italy); MCINN (Spain); SNSB (Sweden); STFC (UK); and NASA (USA).

## REFERENCES

- Bekki K., 2013, MNRAS, 432, 2298  
 Bekki K., 2014a, MNRAS, 438, 444  
 Bekki K., 2014b, MNRAS, 444, 1615  
 Bendo G. J. et al., 2012, MNRAS, 419, 1833  
 Bendo G. J. et al., 2015, MNRAS, 448, 135  
 Bohringer H., Briel U. G., Schwarz R. A., Voges W., Hartner G., Trumper J., 1994, Nature, 368, 828  
 Boquien M. et al., 2011, AJ, 142, 111  
 Boselli A., Gavazzi G., 2006, PASP, 118, 517  
 Boselli A., Lequeux J., Gavazzi G., 2002, A&A, 384, 33  
 Boselli A. et al., 2010, PASP, 122, 261  
 Boselli A., Cortese L., Boquien M., 2014a, A&A, 564, A65  
 Boselli A., Cortese L., Boquien M., Boissier S., Catinella B., Gavazzi G., Lagos C., Saintonge A., 2014b, A&A, 564, A67  
 Boselli A. et al., 2014c, A&A, 570, A69  
 Burstein D., Heiles C., 1982, AJ, 87, 1165  
 Catinella B. et al., 2010, MNRAS, 403, 683  
 Catinella B. et al., 2013, MNRAS, 436, 34  
 Chung A., van Gorkom J. H., Kenney J. D. P., Crowl H., Vollmer B., 2009, AJ, 138, 1741  
 Ciesla L. et al., 2014, A&A, 565, A128  
 Cortese L., Hughes T. M., 2009, MNRAS, 400, 1225  
 Cortese L. et al., 2010a, A&A, 518, L49  
 Cortese L. et al., 2010b, A&A, 518, L63  
 Cortese L., Catinella B., Boissier S., Boselli A., Heinis S., 2011, MNRAS, 415, 1797  
 Cortese L. et al., 2012a, A&A, 540, A52  
 Cortese L. et al., 2012b, A&A, 544, A101  
 Cortese L. et al., 2014, MNRAS, 440, 942  
 di Serego Alighieri S. et al., 2013, A&A, 552, A8  
 Draine B. T., Li A., 2007, ApJ, 657, 810  
 Dwek E., 1998, ApJ, 501, 643  
 Eales S. A. et al., 2010, A&A, 518, L62  
 Eales S. et al., 2012, ApJ, 761, 168  
 Ellison S. L., Simard L., Cowan N. B., Baldry I. K., Patton D. R., McConnell A. W., 2009, MNRAS, 396, 1257  
 Fumagalli M., Krumholz M. R., Prochaska J. X., Gavazzi G., Boselli A., 2009, ApJ, 697, 1811  
 Giovanelli R., Haynes M. P., 1985, ApJ, 292, 404  
 Groves B. A. et al., 2015, ApJ, 799, 96  
 Gunn J. E., Gott J. R. I., 1972, ApJ, 176, 1  
 Haynes M. P., Giovanelli R., 1984, AJ, 89, 758  
 Hewitt J. N., Haynes M. P., Giovanelli R., 1983, AJ, 88, 272  
 Hughes T. M., Cortese L., 2009, MNRAS, 396, L41  
 Hughes T. M., Cortese L., Boselli A., Gavazzi G., Davies J. I., 2013, A&A, 550, A115  
 Issa M. R., MacLaren I., Wolfendale A. W., 1990, A&A, 236, 237  
 Jáchym P., Combes F., Cortese L., Sun M., Kenney J. D. P., 2014, ApJ, 792, 11  
 Kenney J. D., Young J. S., 1986, ApJ, 301, L13  
 Kenney J. D. P., Abramson A., Bravo-Alfaro H., 2015, AJ, 150, 59  
 Lagos C. D. P., Baugh C. M., Lacey C. G., Benson A. J., Kim H.-S., Power C., 2011, MNRAS, 418, 1649  
 Leroy A. K., Walter F., Brinks E., Bigiel F., de Blok W. J. G., Madore B., Thornley M. D., 2008, AJ, 136, 2782  
 McKinnon R., Torrey P., Vogelsberger M., 2016, MNRAS, 457, 3775  
 Magdis G. E. et al., 2012, ApJ, 760, 6  
 Magrini L. et al., 2011, A&A, 535, A13  
 Mouhcine M., Baldry I. K., Bamford S. P., 2007, MNRAS, 382, 801  
 Muñoz-Mateos J. C. et al., 2009, ApJ, 701, 1965  
 Navarro J. F., Frenk C. S., White S. D. M., 1997, ApJ, 490, 493  
 Pappalardo C. et al., 2012, A&A, 545, A75  
 Petropoulou V., Vilchez J., Iglesias-Páramo J., 2012, ApJ, 749, 133  
 Pettini M., Pagel B. E. J., 2004, MNRAS, 348, L59  
 Popping G., Somerville R. S., Trager S. C., 2014, MNRAS, 442, 2398  
 Rémy-Ruyer A. et al., 2014, A&A, 563, A31

- Schindler S., Binggeli B., Böhringer H., 1999, *A&A*, 343, 420  
Schruba A. et al., 2011, *AJ*, 142, 37  
Scott T. C., Usero A., Brinks E., Bravo-Alfaro H., Cortese L., Boselli A., Argudo-Fernández M., 2015, *MNRAS*, 453, 328  
Scoville N. et al., 2014, *ApJ*, 783, 84  
Sivanandam S., Rieke M. J., Rieke G. H., 2010, *ApJ*, 717, 147  
Solanes J. M., Manrique A., García-Gómez C., González-Casado G., Giovanelli R., Haynes M. P., 2001, *ApJ*, 548, 97  
Tonnesen S., Bryan G. L., 2010, *ApJ*, 709, 1203  
Vollmer B., Braine J., Combes F., Sofue Y., 2005, *A&A*, 441, 473  
Vollmer B., Braine J., Pappalardo C., Hily-Blant P., 2008, *A&A*, 491, 455  
Vollmer B., Soida M., Chung A., Chemin L., Braine J., Boselli A., Beck R., 2009, *A&A*, 496, 669  
Zibetti S., Charlot S., Rix H., 2009, *MNRAS*, 400, 1181

This paper has been typeset from a  $\text{\TeX}/\text{\LaTeX}$  file prepared by the author.